Published in final edited form as:
Mol Microbiol. 2014 July ; 93(1): 113–128. doi:10.1111/mmi.12643.

The Bacterial Septal Ring Protein RlpA is a Lytic Transglycosylase that Contributes to Rod Shape and Daughter Cell Separation in *Pseudomonas aeruginosa*

Matthew A. Jorgenson[1], **Yan Chen**[2], **Atsushi Yahashiri**[1], **David L. Popham**[2], and **David S. Weiss**[*,1]

[1]Department of Microbiology, Carver College of Medicine The University of Iowa Iowa City, IA 52242

[2]Department of Biological Sciences Virginia Tech Blacksburg, VA 24061

Summary

Rare lipoprotein A (RlpA) is a widely-conserved outer membrane protein of unknown function that has previously only been studied in *Escherichia coli*, where it localizes to the septal ring and scattered foci along the lateral wall, but mutants have no phenotypic change. Here we show *rlpA* mutants of *Pseudomonas aeruginosa* form chains of short, fat cells when grown in low osmotic strength media. These morphological defects indicate RlpA is needed for efficient separation of daughter cells and maintenance of rod shape. Analysis of peptidoglycan sacculi from an *rlpA* deletion mutant revealed increased tetra and hexasaccharides that lack stem peptides (hereafter called “naked glycans”). Incubation of these sacculi with purified RlpA resulted in release of naked glycans containing 1,6-anhydro *N*-acetylmuramic acid ends. RlpA did not degrade sacculi from wild-type cells unless the sacculi were subjected to a limited digestion with an amidase to remove some of the stem peptides. Thus, RlpA is a lytic transglycosylase with a strong preference for naked glycan strands. We propose that RlpA activity is regulated *in vivo* by substrate availability, and that amidases and RlpA work in tandem to degrade peptidoglycan in the division septum and lateral wall.

Keywords

murein; peptidoglycan hydrolase; divisome; chaining defect; SPOR domain

Introduction

Most bacteria have a peptidoglycan (PG) cell wall that protects the organism from lysis due to turgor pressure and confers on the cell its characteristic shape [reviewed in (Vollmer *et al.*, 2008a)]. The PG sacculus contains a carbohydrate backbone composed of a repeating disaccharide of *N*-acetylglucosamine and *N*-acetylmuramic acid, abbreviated here as NAG and NAM, respectively (Fig. 1). These glycan strands are cross-linked by oligopeptides

[*]To whom correspondence should be addressed. David S. Weiss, Ph.D. The University of Iowa Department of Microbiology 51 Newton Rd, RM 3-372 Iowa City, IA 52242 Phone: 319-335-7785 Fax: 319-335-9006 david-weiss@uiowa.edu..

attached to the NAM moieties. Because the sacculus is a single, covalently-closed molecule that completely surrounds the cell, it must be continually remodeled during growth and cell division. In particular, for rod-shaped bacteria to elongate, PG in the lateral wall must be selectively hydrolyzed to make room for insertion of new material, and selective hydrolysis of septal PG is required for daughter cells to separate after cell division.

Bacteria typically produce multiple, seemingly redundant PG hydrolases that are usually classified by the type of bond they cleave in PG (Fig. 1A) (van Heijenoort, 2011, Vollmer *et al.*, 2008b). These enzymes include amidases that liberate the stem peptides from the glycan backbone, lytic transglycosylases that degrade the glycan backbone, endopeptidases that cleave cross-links between adjacent stem peptides, and carboxypeptidases that trim the ends of stem peptides (Fig. 1A). Whereas the enzymatic activity of the various PG hydrolases is usually clear-cut, their precise physiological roles are often difficult to establish because mutants lacking one or two of these enzymes frequently grow and divide normally. But at least in *E. coli*, mutants lacking larger numbers of PG hydrolases exhibit complex morphological abnormalities (Heidrich *et al.*, 2001, Heidrich *et al.*, 2002, Potluri *et al.*, 2012, Priyadarshini *et al.*, 2007). These observations point to extensive functional redundancy and suggest some hydrolases contribute to both elongation and daughter cell separation. Nevertheless, studies in *E. coli* have highlighted the importance of amidases for daughter cell separation and endopeptidases for elongation (Heidrich *et al.*, 2001, Priyadarshini *et al.*, 2007, Uehara *et al.*, 2010, Singh *et al.*, 2012). Endopeptidases also play a critical role in elongation in *Bacillus subtilis* and *Vibrio cholerae* (Hashimoto *et al.*, 2012, Dörr *et al.*, 2013).

The focus of this manuscript is an outer membrane lipoprotein of previously unknown function named RlpA (rare lipoprotein A), which we show below is an unusual lytic transglycosylase—it preferentially digests “naked” glycan strands that lack stem peptides. Prior to this report, RlpA had only been studied in *E. coli*, where several observations linked the protein to morphogenesis and peptidoglycan metabolism, albeit only in indirect ways. Fusions of mCherry to RlpA revealed localization to scattered foci along the lateral wall (Gerding *et al.*, 2009) and, even more prominently, to the septal ring that mediates cell division (Gerding *et al.*, 2009, Arends *et al.*, 2010). In *E. coli rlpA* is in an operon with *pbpA* and *rodA*, which encode proteins needed for peptidoglycan synthesis during elongation (Fig. 2A) (Matsuzawa *et al.*, 1989, Mohammadi *et al.*, 2011, Banzhaf *et al.*, 2012). Immediately downstream but transcribed separately is *dacA*, which codes for a peptidoglycan hydrolase implicated in spatial control of cell division (Fig. 2A) (Potluri *et al.*, 2012). The sequence of RlpA contains two domains, a C-terminal “SPOR domain” (Pfam 05036) and a central “RlpA-like double psi beta barrel domain” (DPBB; Pfam 03330) (Fig. 2B) (Punta *et al.*, 2012). SPOR domains are about 75 amino acids long, bind peptidoglycan, and localize to the septal ring (Ursinus *et al.*, 2004, Möll & Thanbichler, 2009, Gerding *et al.*, 2009, Arends *et al.*, 2010). Most characterized SPOR domain proteins are involved in cell division, although at least two are involved in other aspects of morphogenesis (Mishima *et al.*, 2005, Gode-Potratz *et al.*, 2011). DPBB folds are found in many proteins and are often enzymatic, but the activity is different in different proteins [reviewed in (Castillo *et al.*, 1999)]. Threading the DPBB domain from *E. coli* RlpA by the Protein Homology/analogy

Recognition Engine (PHYRE) (Kelley & Sternberg, 2009) revealed distant similarity to expansin-like cellulose binding domains (which bind carbohydrates but are not enzymatic (Sampedro & Cosgrove, 2005)) and to the MltA lytic transglycosylase of *E. coli* (van Straaten *et al.*, 2005). Neither of these similarities is strong enough to be detected in a BLAST search.

Collectively, these observations suggest RlpA might be an enzyme involved in synthesis or degradation of PG during division and/or elongation, but *E. coli* null mutants of *rlpA* do not have any obvious morphological defects (Gerding *et al.*, 2009, Arends *et al.*, 2010). Moreover, in our hands purified RlpA from *E. coli* does not digest PG sacculi isolated from wild-type cells. What broke this impasse was the fortuitous observation that in *P. aeruginosa* an *rlpA* null mutant has striking morphological defects that link the protein to division and rod shape. Follow-up studies revealed P. *aeruginosa* RlpA is a lytic transglycosylase whose activity appears to be restricted to “naked” glycan strands that lack stem peptides.

Results

An *rlpA* mutant has a chaining phenotype in *P. aeruginosa*

RlpA appears to be the most highly conserved of all the SPOR domain proteins, with over 5000 examples from more than 2,500 species listed in the Pfam database (version 27.0) (Punta *et al.*, 2012). Conservation is usually a hallmark of importance, yet of the four SPOR domain proteins in *E. coli*, RlpA is the only one that appears to be completely dispensable (Gerding *et al.*, 2009, Arends *et al.*, 2010). We therefore decided to analyze RlpA in other bacterial species in hopes of finding a useful phenotype. Utilizing the BLAST function on the *Pseudomonas* Genome Database website (Winsor *et al.*, 2011), we identified *rlpA* in strain PA14 as PA14_12090. The E-value for comparison of the *E. coli* and *P. aeruginosa* RlpA proteins is 10^{-24}. The two proteins are very similar in overall size and domain structure (Fig. 2B). In both organisms *rlpA* appears to be cotranscribed with genes involved in biogenesis of the PG sacculus (Fig. 2A), but there is one striking difference— the gene immediately upstream of *rlpA* in *P. aeruginosa* encodes a soluble lytic transglycosylase designated *sltb1*that is not found in the *E. coli* operon (Blackburn & Clarke, 2002, Nikolaidis *et al.*, 2012).

The PA14 transposon insertion library contains a single insertion mutation of *rlpA* (*rlpA*::Tn); the insertion site is 138 base pairs downstream of the first T in the TTG start codon (http://ausubellab.mgh.harvard.edu/cgi-bin/pa14/home.cgi) [11, December 2013] (Liberati *et al.*, 2006). We obtained the *rlpA*::Tn mutant, confirmed the insertion site by PCR, and tested its phenotypes under various growth conditions. The mutant grew normally on LB plates containing 10 g/L NaCl, but, to our surprise, was not viable when plated on LB lacking NaCl (hereafter designated LB0N) over a range of temperatures (shown for 37°C in Fig. 2C). The *rlpA*::Tn mutant appeared normal in LB broth, but in LB0N it grew slowly and formed chains of unseparated cells (Fig. 2D). These phenotypes did not result from polarity onto *dacC* because a *dacC*::Tn mutant (from the same mariner insertion library) had a similar plating efficiency to wild type on LB0N plates and the cells looked normal when grown in LB0N broth (Fig. 2C and 2D).

We then constructed an in-frame deletion of *rlpA*, which phenocopied the *rlpA*::Tn mutant. Specifically, the Δ*rlpA* mutant was indistinguishable from wild type when grown in LB broth (Fig. 2E), but growth arrested about 2.5 hours after shift to LB0N broth (Fig. 2F) and the mutant failed to form colonies when plated on LB0N (Fig. 2C). Microscopy of cells grown in LB0N broth confirmed a chaining defect, which became more pronounced the longer the cultures were allowed to grow (Fig. 2D and 3B). Close inspection of cells in the chains revealed they were ~50% shorter and 20% fatter than wild type (Table 1). Analysis of cells in the chains by fluorescence loss in photobleaching (FLIP) revealed 84% of the septa were closed, indicating that membrane constriction had gone to completion (Fig S1A). The morphological and viability defects could be rescued by expressing *rlpA* from a plasmid (Fig. 2C and 2D). The mutant could also be rescued by replacing NaCl in the growth medium with proline or sucrose (Fig. S1B), indicating the phenotypic changes are due to a general osmotic stress rather than specifically related to NaCl. Time-lapse microscopy of live cells in LB0N spotted on an agarose pad revealed about half of the cells lysed, while the other half stopped growing but remained phase dark (Fig. S1C). Collectively, our findings demonstrate that RlpA is important for daughter cell separation and rod shape when *P. aeruginosa* is grown in medium of low osmotic strength.

Septal localization of *P. aeruginosa* RlpA

To explore localization of the *P. aeruginosa* protein, we replaced the chromosomal *rlpA* allele with an *rlpA-mCherry* gene fusion. Western blotting with anti-mCherry sera indicated the fusion protein was stable (Fig. 4A). The RlpA-mCherry fusion protein was functional as evidenced by viability on LB0N plates (Fig. 4B) and absence of chaining in LB0N broth (Fig. 5A-C; Table S1). Fluorescence microscopy of live cells grown to midlog phase in LB revealed septal localization in ~42% of the cells in the population (n > 500 cells; Fig. S1D). Most of these cells had obvious constrictions, suggesting RlpA is a late recruit to the septal ring. Polar localization was observed in ~15% of the cells (Fig. S1D). Because most of these cells were short, we suspect this reflects persistence of RlpA-mCherry after division is complete. Finally, we observed weak foci along the lateral wall in ~5% of the cells, which might reflect a role for RlpA in elongation, peptidoglycan recycling or tailoring of the lateral wall. In total, the localization patterns seen in *P. aeruginosa* are similar to what has been reported in *E. coli* (Gerding *et al.*, 2009, Arends *et al.*, 2010).

To determine if the SPOR domain is needed to target RlpA to the midcell, we replaced the chromosomal allele of *rlpA* with an *rlpA*(ΔSPOR)-*mCherry* construct. The fusion protein was stably produced (Fig. 4A) and functional (Fig. 4B; Table S1), but septal localization was barely detectable and foci were no longer observed along the lateral wall (Fig. 5D). Thus, the SPOR domain of RlpA is very important for normal localization, but not for cell division or rod shape. This paradoxical situation has been reported previously for FtsN, which is targeted to the division site by its SPOR domain but nevertheless supports cell division even after the SPOR domain has been deleted (Ursinus *et al.*, 2004, Möll & Thanbichler, 2009, Gerding *et al.*, 2009). The most plausible interpretation is that small amounts of properly localized RlpA are sufficient for biological function.

Low osmolarity does not induce *rlpA*

Because the *rlpA-mCherry* fusion was integrated into the native locus, we used it to ask whether *rlpA* expression is osmo-regulated. Essentially identical steady-state levels of RlpA-mCherry protein were detected by Western blotting with anti-mCherry when cells were grown in LB or LB0N (Fig. S2). Thus, although osmotic stress is needed to uncover the phenotypes associated with loss of *rlpA*, the gene does not appear to be part of an osmotic stress response regulon.

PG from the Δ*rlpA* mutant is enriched in naked glycans

The chaining phenotype suggested RlpA is a PG hydrolase, but we were unable to detect hydrolase activity when purified RlpA was incubated with sacculi isolated from wild-type cells, despite exploring a number of assay formats (documented below). We therefore turned to analysis of the PG in hopes of identifying structural abnormalities that would provide some insight into what RlpA does. For these experiments wild type and the Δ*rlpA* mutant were grown for several generations in LB0N until the mutant had formed chains 4-8 cells in length. Comparison of the HPLC elution profiles of muropeptides obtained after muramidase digestion of sacculi revealed several differences, the most striking of which were that the mutant was enriched in three muropeptides that eluted from the HPLC column with retention times of 15 min (P5), 23 min (P9) and 29 min (P13) (Fig. 6, Table 2). The peaks were identified using a combination of amino sugar analysis, amino acid analysis and mass spectrometry methods (Table S2 and S3).

The species eluting as P5 contained abundant NAG and NAM but little in the way of amino acids, suggesting it is a fragment of the glycan backbone that lacks peptide side chains. The P5 product had a mass-charge ratio (*m/z*) of 999.4 Da, consistent with it being the tetrasaccharide NAG-NAM-NAG-NAMol (abbreviated TS, predicted *m/z* = 999.5 Da; the terminal NAM is in the alcohol form due to borohydride reduction). This was confirmed by fragmentation analysis with tandem mass spectrometry (Table S3). The P9 product was also highly enriched in amino sugars as compared to amino acids, and had a mass-charge ratio of 1477.6 Da, consistent with the hexasaccharide NAGNAM-NAG-NAM-NAG-NAMol (abbreviated HS, predicted *m/z* = 1477.6). Finally, the P13 product had excess amino sugars as compared to amino acids, but the ratio was not as skewed as for the other two products. The mass-charge ratio was 1442.9, consistent with a tetrasaccharide that contains one tetrapeptide side-chain: NAG-NAM-NAG-NAMol-Ala-Glu-Dpm-Ala (abbreviated TS-Tetra, predicted *m/z* = 1442.6 Da). This structure for the P13 product was consistent with at least 9 fragments in tandem mass spectrometry (Table S3). The fact that we recovered tetra- and hexasaccharide fragments indicates mutanolysin does not cleave very efficiently at NAM residues that lack stem peptides. A lack of mutanolysin digestion adjacent to a peptide-free NAM within a tetrasaccharide was previously observed (Gilmore *et al.*, 2004). Mutanolysin also fails to cut at muramic δ–lactam (Popham *et al.*, 1996a), a modified form of NAM that also lacks a stem peptide and is abundant in bacterial spore PG (Warth & Strominger, 1969). Thus, when doing muropeptide analysis of PG it is not safe to assume that all fragments have been reduced to disaccharides.

Besides the above-mentioned muropeptides that were more abundant in the mutant, two muropeptides were less abundant (Fig. 6, Table 2). These eluted at 14 min (P4) and 22 min (P8), and proved to be disaccharides with a tripeptide or pentapeptide sidechains, respectively. We do not know the significance of these changes, which in any event were small compared to the increases in the P5, P9 and P13 muropeptides.

In summary, PG from the Δ*rlpA* mutant accumulated regions of glycan strand that lack stem peptides. This finding suggested RlpA degrades naked glycans and explained why RlpA failed to exhibit hydrolase activity in our *in vitro* assays, because sacculi from wild-type cells are essentially devoid of naked glycans (Fig. 6, Table 2).

RlpA is an unusual lytic endo-transglycosylase with specificity for glycan strands that lack stem peptides

For enzymological assays we purified a soluble derivative of RlpA that carried a hexahistidine tag in place of the N-terminal type II signal sequence (His_6-RlpA). As substrate we prepared PG sacculi that had been labeled with the dye Remazol Brilliant Blue R (RBB-PG) (Zhou *et al.*, 1988). Although His_6-RlpA did not have convincing hydrolase activity when incubated with RBB-PG sacculi from wild-type cells (as expected), it readily hydrolyzed sacculi from the Δ*rlpA* mutant (Fig. 7A and B). This was confirmed using muropeptide analysis to examine the effect of incubating His_6-RlpA with unlabeled sacculi. In the case of sacculi from wild-type cells, no PG fragments were released into the soluble fraction, and analysis of the residual insoluble pellet indicated it was not changed relative to the starting material (Fig S3). But when His_6-RlpA was incubated with sacculi from the *rlpA* mutant, P5 (tetrasaccharide) and to a lesser extent P9 (hexasaccharide) disappeared from the insoluble fraction and two products appeared in the supernatant (Fig. 7C and Fig. S3). These products eluted from the HPLC column at 33 min (Peak a) and 43 min (Peak b). The first product was identified by mass spectrometry as a tetrasaccharide with a 1,6-anhydro end: NAG-NAM-NAG-1,6-anhydroNAM (observed *m/z* = 979.3 Da, predicted = 979.4 Da). Similarly, the second product was identified as a hexasaccharide with a 1,6-anhydro end: NAG-NAM-NAG-NAM-NAG-1,6-anhydroNAM (observed *m/z* = 1457.8 Da, predicted = 1457.5 Da). These identifications were confirmed by the observation of appropriate fragmentation products during tandem mass spectrometry (Table S4). Moreover, the HPLC retention time was not affected by treatment with the reducing agent $NaBH_4$ (Fig. 7C), consistent with the presence of a non-reducible 1,6-anhydroNAM end. The presence of 1,6-anhydroNAM ends in the cleavage products indicates RlpA is a lytic transglycosylase rather than a muramidase or glucosamidase (Höltje *et al.*, 1975, Vollmer *et al.*, 2008b). The relatively large size of the released products (tetra- and hexasaccharides) indicates RlpA is an “endo” enzyme that cuts in the middle of glycan chains rather than an “exo” enzyme that cuts near the end of glycan chains to release disaccharides. We purified sufficient P5 (tetrasaccharide) to use as a substrate for His_6-RlpA, but no hydrolysis was detected, suggesting RlpA requires greater context before cleaving (Fig. S4).

Several aspects of the assays shown in Figure 7 need to be clarified to prevent potential points of confusion. The reason His_6-RlpA can almost completely solubilize dye-labeled sacculi in Figure 7B despite having very limited substrate specificity is that much of the

"soluble" PG is in the form of very large fragments that remain in the supernatant when samples are centrifuged for 10 min to pellet residual insoluble sacculi. This also accounts the apparent discrepancy between extensive solubilization on the one hand and the recovery of only a small amount of soluble products after HPLC on the other (Fig. 7B vs. 7C). Most of the "soluble" PG fragments released during RlpA treatment are too large for HPLC analysis, which in Figure 7C did not include a muramidase digestion step. Consistent with this, if the soluble fraction is treated with muramidase prior to loading onto the HPLC column, we observe more total material and a variety of muropeptide structures (data not shown). Finally, the inference that RlpA is lytic transglycosylase is only valid if the 1,6-anhydroNAM ends were introduced by RlpA cleavage. We infer that the 1,6-anhydroNAM ends were introduced by RlpA cleavage because they are too abundant to be accounted for by muramidase-like endolytic release of short glycans that contained preexisting 1,6-anhydroNAM ends. Note that RlpA digestion of sacculi from the Δ*rlpA* mutant greatly diminished the abundance of tetra- and hexasaccharides that *lack* 1,6-anhydroNAM ends (Fig. 7C, peaks 5 and 9) while at the same time releasing tetra- and hexasaccharides that *contain* 1,6-anhdyroNAM ends (Fig 7C, peaks a and b). We take these findings to mean Δ*rlpA* sacculi contained longer naked glycans that were cleaved by muramidase to produce oligosaccharides with NAM ends or by RlpA to produce oligosaccharides with 1,6-anhydroNAM ends.

RlpA degrades the product of amidase digestion

These results suggest RlpA degrades the carbohydrate backbone of PG only after amidases have removed stem peptides. This is unusual, but has been reported previously for SpoIID of *Bacillus subtilis* (Morlot *et al.*, 2010) and MltE of *E. coli* (Kraft *et al.*, 1998), although some reports indicate these enzymes also cleave glycans that have stem peptides under some circumstances (Kraft *et al.*, 1998, Gutierrez *et al.*, 2010, Lee *et al.*, 2013). In a recent study of SpoIID (Morlot *et al.*, 2010), the purified protein only degraded the glycan backbone if the reaction mixtures included an amidase to remove stem peptides. We used a modified version of that assay to show the same is true of RlpA. RBB-labeled sacculi from wild type cells were subjected to a limited digestion with His_6-AmiD from *E. coli*, then the enzyme was inactivated by heating to 95°C. Upon addition of His_6-RlpA, robust dye release was observed; in four independent replicates AmiD treatment stimulated RlpA activity by 5.7 ± 2.1 fold (mean ± standard deviation) (Fig. 8A and C, Fig. S5). Conversely, pre-treatment of wild-type sacculi with His_6-RlpA did not stimulate subsequent hydrolysis by His_6-AmiD (Fig. 8B and C, Fig. S5). The fact that stimulation depended on the order of addition indicates dye release is not simply a consequence of the cumulative activity of the two enzymes but instead means that AmiD creates the substrate cleaved by RlpA.

Residue D157 in the DPBB is critical for lytic transglycosylase activity

We used Clustal Omega (Sievers *et al.*, 2011) to create a multiple sequence alignment of DPBB domains from various RlpAs and identified highly conserved amino acids (Fig. S6A). Based on this alignment, we constructed the following four mutant variants: E120A, D123A, H131A and D157N. The mutant derivatives were purified and tested for lytic transglycosylase activity in the dye release assay with Δ*rlpA* sacculi as substrate. Dye release activity was greatly reduced in every case, indicating the targeted residues are

important for lytic transglycosylase activity (Fig. 7B). In particular, the D157N protein had no detectable enzymatic activity.

To assess the importance of these residues for RlpA function *in vivo*, the mutant derivatives were fused to *mCherry* and recombined into the native *rlpA* locus. All of the mutant proteins were produced in normal amounts and localized to the septal ring (Fig. 4A, Fig. 5E-H), but only the D157N lesion phenocopied the Δ*rlpA* mutant—it failed to support growth on LB0N plates (Fig. 4B) and microscopy revealed chains of short, fat cells when grown in LB0N broth (Fig. 5H and Table S1). The second most defective protein in the dye release assay, the E120A mutant, resulted in slightly increased chaining as compared to wild type (Table S1). Collectively, these findings imply the enzymatic activity of RlpA is important for proper growth and division but low levels of activity are sufficient. If the results from the dye-release assay can be taken at face value, it appears that the break-point is around 6% of wild-type activity (i.e., the activity of the E120A protein). This is consistent with the observation that the ΔSPOR domain variant of RlpA supports proper growth and division even though it does not localize very efficiently to the midcell (Fig. 5). It should be noted that *P. aeruginosa* has 9 additional lytic transglycosylases, some of which might compensate for lack of RlpA (Legaree & Clarke, 2008).

Evidence that RlpA is not needed for proper function of SltB1, MltB1 or AmiB

Early on during this investigation we had observed that RlpA is needed for efficient daughter cell separation, but purified RlpA did not appear to be a PG hydrolase, so we invested some effort in in exploring whether RlpA activates or recruits a PG hydrolase. Although this line of investigation was abandoned once we discovered that RlpA had a lytic transglycosylase activity, we had by that time learned some new things about three *P. aeruginosa* PG hydrolases: SltB1, MltB1 and AmiB.

We first investigated the lytic transglycosylases SltB1 and MltB1 (Blackburn & Clarke, 2002, Scheurwater *et al.*, 2007, Cavallari *et al.*, 2013). These enzymes were chosen because *sltB1* is adjacent to *rlpA* (Fig. 2A) and MltB1 is ~40% identical to SltB1. We constructed in-frame deletions of *sltB1* and *mltB1*, and observed that both mutants exhibited normal morphology when grown in LB, as previously reported (Blackburn & Clarke, 2002). More importantly for our purposes, morphology was also normal in LB0N (Fig. S7A). Even a Δ*sltb1*Δ*mltb1* double mutant appeared normal in both media (Fig. S7A). We conclude that the phenotypic changes caused by loss of RlpA cannot be explained by failure to activate SltB1 and MtlB1.

We then turned our attention to amidases, because amidase mutants of *E. coli* have chaining and shape defects similar to *rlpA* mutants of *P. aeruginosa* (Heidrich *et al.*, 2001, Priyadarshini *et al.*, 2007). Moreover, AmiB and AmiC localize to the septal ring in *E. coli* (Bernhardt & de Boer, 2003, Peters *et al.*, 2011). Consistent with this, a *P. aeruginosa* AmiB-mCherry fusion protein localized sharply to the septal ring, but this did not require RlpA (Fig. S7B). Therefore, the morphological defects observed in our Δ*rlpA* mutant are not due to failure to recruit AmiB to the septal ring. Nevertheless, AmiB is probably involved in daughter cell separation in *P. aeruginosa* and might work together with RlpA. We also attempted to localize AmiA of *P. aeruginosa* but our fusions to GFP and mCherry were

retained in the cytoplasm (data not shown). It is likely that AmiA localizes to septal regions because, in spite of its name, AmiA of *P. aeruginosa* corresponds to the septal ring amidase AmiC of *E. coli*.

Discussion

Having failed to find a phenotype for a Δ*rlpA* mutation in *E. coli*, we turned to *P. aeruginosa*. We chose this organism not because we had any reason to expect a different outcome, but because an *rlpA*::Tn mutant was readily available (Liberati *et al.*, 2006). Interestingly, the *rlpA*::Tn mutant formed chains of short, fat cells when grown in LB lacking NaCl. Follow-up studies revealed RlpA is a lytic transglycosylase and contributes to both daughter cell separation and rod shape when *P. aeruginosa* is grown in media of low osmotic strength. Further studies will be needed to determine why loss of RlpA does not cause a similar phenotype in *E. coli*, but we anticipate RlpA will prove to be important in many bacteria. In support of this, RlpA is well-conserved, with over 5,000 examples from more than 2,500 species in the Pfam database (Punta *et al.*, 2012). Moreover, Chaput *et al.* reported that a Tn insertion in *mltD* of *Helicobacter pylori* caused a chaining phenotype, but an in-frame deletion of *mltD* did not (Chaput *et al.*, 2007). Intriguingly, the gene immediately downstream of *mltD* is *rlpA*.

RlpA is a new lytic transglycosylase with an unusual specificity for naked glycans

Most characterized lytic transglycosylases solubilize whole PG sacculi because they can efficiently cleave glycan strands containing stem peptides (Vollmer *et al.*, 2008b, Scheurwater *et al.*, 2008, Lee *et al.*, 2013). In contrast, in the case of RlpA we only observe cleavage of glycan strands that lack peptide side-chains, although it should be noted that a weak activity towards glycans that have stem peptides cannot be excluded at this point because we do not know the detection limits of our assays. The substrate preference of RlpA implies it digests glycan strands that have already been processed by cell wall amidases, supporting the view that amidases are the pacemakers for cell separation (Heidrich *et al.*, 2001, Uehara *et al.*, 2010, Uehara & Bernhardt, 2011). The molecular basis for RlpA's unusual specificity will require further investigation. It could arise from the SPOR domain, which probably binds naked glycan strands (Ursinus *et al.*, 2004, Gerding *et al.*, 2009). Alternatively, or in addition, the enzymatic domain may be highly specific. This would account for the ability of RlpA to support normal growth and division even after the SPOR domain is deleted (Fig. 5) and would also explain why RlpA does not lyse cells when overproduced (data not shown).

The specificity of RlpA has implications for two long-standing questions about PG hydrolases in general (Vollmer *et al.*, 2008b, Uehara & Bernhardt, 2011). The first question is, how do the various PG hydrolases work together to facilitate growth and division? Our findings indicate RlpA and the amidases cleave PG in an ordered and sequential fashion—first the amidases remove stem peptides, then RlpA degrades the residual glycan backbone (Fig. 1B). The second general question one must ask of all PG hydrolases is what holds them in check so that they do not inadvertently cause lysis? We think RlpA cannot lyse cells on account of its very limited substrate specificity. Moreover, the activity of RlpA is

regulated on at least two levels—by the SPOR domain, which recruits the protein to the septal ring and by the amidases, whose activity is regulated by a host of septal ring-associated proteins (Uehara *et al.*, 2010, Yang *et al.*, 2011, Yang *et al.*, 2012).

Models for how RlpA could facilitate daughter cell separation and maintenance of rod shape

Cell wall amidases are widely considered the most important enzymes for daughter cell separation, while the endopeptidases are generally thought to be the key enzymes for elongation (Heidrich *et al.*, 2001, Priyadarshini *et al.*, 2007, Hashimoto *et al.*, 2012, Dörr *et al.*, 2013, Singh *et al.*, 2012). Nevertheless, our study of RlpA is not the first to implicate lytic transglycosylases in these processes as well. For example, an *E. coli* mutant lacking three lytic transglycosylases (Δ*mltCDE*) has a mild chaining phenotype, while a mutant lacking six (Δ*slt*Δ*mltABCDE*) has a stronger chaining phenotype—and the cells become short and coccoid, indicating that lytic transglycosylases are important not only for division but also for proper biogenesis of the lateral wall (Heidrich *et al.*, 2002). Chaining has also been reported for a Δ*mltC*Δ*mltE* double mutant in *Salmonella enterica* (Monteiro *et al.*, 2011) and a single deletion of *ltgC* (*E. coli mltA* homolog) in *Neisseria gonorrhoeae* (Cloud & Dillard, 2004). These findings, together with the phenotypes reported here for Δ*rlpA*, suggest many lytic transglycosylases play important roles in daughter cell separation and maintenance of cell shape.

But why? Most current models of the PG sacculus indicate the glycan strands run roughly perpendicular to the long axis of the cell (Vollmer & Höltje, 2004, Gan *et al.*, 2008), although a recent study indicates the glycan strands are not so highly organized (Turner *et al.*, 2013). In the standard model, it would seem amidase activity should be sufficient for separation of daughter cells, so it is not obvious how a lytic transglycosylase would help this process, all the more so in the case of RlpA, which probably only digests PG that has already been cut by an amidase. We suggest that if the division plane and glycan strands are not perfectly aligned, the glycan stands will cross the division plane and be shared by daughter cells, leading to a situation in which both amidases and lytic transglycosylases are needed for efficient daughter cell separation. Likewise, irregularities in the organization of the PG might make efficient elongation dependent upon removal of glycan strands rather than simply breaking crosslinks. Alternatively, RlpA might affect cell separation and rod shape less directly by contributing to PG recycling, tailoring the cell wall, or as part of multiprotein complex that do not function well when RlpA is missing or defective.

Comparison to MltE and SpoIID

Our findings bring to three the number of unique lytic transglycosylases known to be exclusively or primarily active on glycan strands that lack stem peptides: MltE of *E. coli* (Kraft *et al.*, 1998), SpoIID of *B. subtilis* (Morlot *et al.*, 2010) and RlpA of *P. aeruginosa*. Curiously, these three proteins are not homologous to one another and probably have completely different folds, yet they all employ either a glutamate (MltE, SpoIID) or an aspartate (RlpA) as the general acid/base during catalysis (Morlot *et al.*, 2010, Artola-Recolons *et al.*, 2011, Fibriansah *et al.*, 2012). Both MltE (Kraft *et al.*, 1998) and RlpA (Fig. 7C) are “endo” lytic transglycoslyase that cleave internal to glycan chains, whereas SpoIID

is an “exo” enzyme that releases disaccharides from the end of glycan (Morlot *et al.*, 2010). SpoIID is part of a protein complex required for the engulfment step of sporulation, and works together with SpoIIP, a cell wall amidase that is part of the same complex (Abanes-De Mello *et al.*, 2002, Chastanet & Losick, 2007). Whether MltE in *E. coli* and RlpA in *P. aeruginosa* have a dedicated amidase is not known, but AmiB is a likely partner for RlpA in view of our finding that both proteins localize to the division site.

Potential new insights into MltA, a bacterial “expansin”, and a protein of unknown function

Structural modeling using Phyre (version 2.0) revealed the catalytic DPBB domain of RlpA has intriguing similarity to several proteins in the structure databases. One of these is the lytic transglycosylase MltA of *E. coli* (PDB 2AE0; (van Straaten *et al.*, 2005)), which has been reported to be equally active on glycan strands with and without stem peptides (Romeis *et al.*, 1993, Ursinus & Höltje, 1994). The relatively high activity of MltA on naked glycan strands is interesting in light of its distant structural relationship to RlpA, which is specific for this substrate. The catalytic site of MltA contains two highly conserved aspartates, D297 and D308, both of which are important for catalysis, especially D308, which acts as the general acid/base (van Straaten *et al.*, 2005, Powell *et al.*, 2006, van Straaten *et al.*, 2007). These residues align with the conserved residues D157 and D168 of *P. aeruginosa* RlpA, suggesting D168 is the catalytic acid/base (Fig. S6). But in *E. coli* RlpA this residue is a serine (Fig. S6B), and our data indicate D157 of the *P. aeruginosa* protein is important for lytic transglycosylase activity (though we have yet to test D168). Further work will be needed to determine what role the conserved aspartates play in RlpA and whether the *E. coli* protein has enzyme activity. According to the Phyre model of RlpA on MltA, none of the other amino acids we targeted for mutagenesis in RlpA are in the catalytic pocket, although some are close.

RlpA also showed similarity to YoaJ from *B. subtilis* (PDB 3D30; (Kerff *et al.*, 2008)). YoaJ is reported to be an expansin (Kerff *et al.*, 2008), a class of proteins found mainly in plants. Expansins are not catalytic but bind cellulose and loosen its structure (Sampedro & Cosgrove, 2005). The report (Kerff *et al.*, 2008) that concluded YoaJ is an expansin considered the possibility that it is a PG hydrolase but ruled this out because (i) the purified protein did not digest PG sacculi *in vitro* and (ii) a *B. subtilis yoaJ* null mutant did not have an abnormal morphology. Interestingly, Phyre models superimpose D71 of YoaJ with D157 of RlpA and D82 of YoaJ with D308 of MltA (Fig. S6B). We suggest YoaJ might be a PG hydrolase, but like RlpA, it only digests naked glycan strands and is only needed for proper morphology under a limited set of growth conditions.

The best match returned by Phyre is to a protein of unknown function from *P. aeruginosa* PAO1 designated PA4485 (PDB 4AVR; (Moynie *et al.*, 2013)). Similar to RlpA, PA4485 is a predicted outer membrane lipoprotein that contains a DPBB fold, but unlike RlpA does not contain a SPOR domain. Both catalytic aspartates (as inferred from RlpA and MltA) are present in PA4485, suggesting it is a lytic transglycosylase. Neither the PAO1 nor the PA14 transposon library (Jacobs *et al.*, 2003, Liberati *et al.*, 2006) contains transposon insertions in *PA4485*, raising the possibility that PA4485 might be essential, although this would be unprecedented for a lytic transglycosylase.

Materials and Methods

Media

Unless otherwise noted, *E. coli* and *P. aeruginosa* strains were grown in Luria-Bertani (LB) media containing 0.5% yeast extract, 1% tryptone and 1% NaCl. Plates contained 1.5% agar. When necessary, ampicillin (Amp), carbenicillin (Carb), gentamicin (Gent), irgasan (Irg), and kanamycin (Kan) were used at 200, 300, 100, 25 and 40 μg/mL, respectively.

Strains and plasmids

All strains, plasmids and primers used in this study are listed in Tables S5, S6 and S7, respectively. All plasmids used for *in vivo* experiments are derivatives of pJN105 (Newman & Fuqua, 1999). Amino acid substitutions in the DPBB domain of RlpA were generated using a multistep PCR procedure involving megapriming (Kwok *et al.*, 1994). Plasmids for overproducing hexahistidine (His_6-) tagged RlpA variants are derivatives of pQE-80L (Qiagen). All strains used for *in vivo* experiments are derivatives of *P. aeruginosa* strain UCBPP- PA14. All deletion constructs were generated using plasmid pEXG2 as previously described (Rietsch *et al.*, 2005). pEXG2 derivatives were transferred from derivatives of *E. coli* strain SM10 to wild type PA14 by conjugation as described (Schweizer, 1992) except that Irg was used to counter select against the *E. coli* donor strain because a Δ*rlpA* mutant is not viable on the (low osmolarity) minimal-citrate media often used to counter select *E. coli* after such matings. Resolution of the co-integrant was selected for on LB0N plates containing 5% sucrose (~150 mM, which allows for growth of the Δ*rlpA* mutant in the absence of NaCl).

Protein purification

Wild type and mutant His_6-RlpA proteins were overproduced in *E. coli* BL21 and purified at 4°C by cobalt affinity chromatography per the manufacturer's instructions (Clontech). Cells were grown at 30°C to an OD_{600} ~0.5 and protein production was induced with 1 mM isopropyl-ß-D-thiogalactoside (IPTG) for three hours. The purified proteins were dialyzed into storage buffer (25 mM HEPES, 150 mM NaCl, 5% glycerol, pH 7.0) at 4°C and aliquots were stored at -80°C until needed. Typical yields were10 mg from a 500 mL culture as determined by UV-VIS spectrometry using a NanoDrop-1000 spectrophotometer (Thermo Scientific) and purity was judged to be ~95% by sodium dodecyl sulfate polyacrylamide gel electrophoresis (SDS-PAGE). His_6-AmiD was purified essentially as described and stored at -80°C (Uehara & Park, 2007). The purity was ~95% as judged by SDS-PAGE.

Morphology of *dacC, mltb1, rlpA* and *sltb1* mutants

Overnight cultures grown in LB were adjusted to an OD_{600} ~0.05 (~1:100 dilution) in the same medium and grown to an OD_{600} ~1.0 at 37°C. Cultures were then diluted to an OD_{600} ~0.05 in LB0N medium and grown to an OD_{600} ~0.5 at which point the cells were fixed as described except that glutaraldehyde was omitted (Pogliano *et al.*, 1995). Cells were stained with the membrane dye FM4-64 (Invitrogen) to better visualize chaining.

Rescue of *rlpA* and *dacC* mutants

Overnight cultures were adjusted to OD_{600} = 1.0 and plating efficiency was assessed by spotting tenfold serial dilutions onto LB or LB0N plates (Arends *et al.*, 2010). Plates were incubated for 18 hours at 37°C and then photographed.

Scanning electron microscopy (SEM)

Overnight cultures grown in LB were matched to an OD_{600} ~0.01 in the same medium and grown to an OD_{600} ~1.0 at 37°C. Cultures were then diluted to an OD_{600} ~0.1 in LB0N medium and grown to an OD_{600} ~0.7 at which point the cells were fixed with 2.5% glutaraldehyde in 0.1 M sodium cacodylate buffer and prepared essentially as previously described (Hsiao *et al.*, 2011). Samples were examined by an S-4800 field emission scanning electron microscope (Hitachi High Technologies America Inc.). All electron microscopy was performed at the University of Iowa Central Microscopy Research Facility.

Protein localization and microscopy

Strains expressing mCherry fusion proteins were grown overnight in LB, adjusted to an OD_{600} = 0.02 (~1:200 dilution) in the same medium and grown at 37°C to an OD_{600} ~1.0. Cultures were then diluted to an OD_{600} ~0.1 in LB0N and grown to an OD_{600} ~0.5 after which 4 μl were spotted onto 1% agarose pads and visualized by phase-contrast and fluorescence microscopy (Tarry *et al.*, 2009). For imaging mCherry fusions we used a filter for Texas Red (Chroma no. U-N41004). Our microscope, camera and software have been previously described (Mercer & Weiss, 2002).

FLIP experiments

Cells expressing cytoplasmic GFP from pMRP9-1 (Davies *et al.*, 1998) were grown overnight at 37°C in LB containing carbenicillin and diluted 1:100 in the same medium and grown to an OD_{600} ~1.0. Cultures were then diluted 1:10 in LB0N containing carbenicillin and grown to an OD_{600} = 0.5 after which 4 μL were spotted onto 1% agarose pads. A coverslip was placed over the sample and sealed with nail polish. Fluorescence loss in photobleaching (FLIP) was then performed using a Zeiss LSM 510 confocal microscope essentially as described (Priyadarshini *et al.*, 2007). All confocal microscopy was performed at the University of Iowa Central Microscopy Research Facility.

Preparation of PG and labeling with RBB

Whole PG sacculi were isolated from 1-liter cultures as previously described (Arends *et al.*, 2010). Overnight cultures of *P. aeruginosa* strains grown in LB were diluted to an OD_{600} ~0.05 in the same medium and grown to an OD_{600} ~1.0 at 37°C. Cultures were then diluted to an OD_{600} ~0.05 in LB0N and grown for three hours (OD_{600} ~0.5-0.6) before harvest. Remazol Brilliant Blue (RBB) labeling of PG was performed essentially as previously described (Uehara *et al.*, 2010, Zhou *et al.*, 1988). Purified sacculi were incubated with 20 mM RBB in 0.25 M NaOH overnight at 37°C. Reactions were neutralized by the addition of HCl and RBB-PG was collected by centrifugation at 18,000 × g for 15 min. Pellets were washed repeatedly with water until the supernatants were colorless. RBB-labeled sacculi were stored in water at 4°C until needed.

The dye-release assay for RlpA activity

A standard 100 μL reaction mixture contained PBS buffer (137 mM NaCl, 3 mM KCl, 9 mM NaH_2PO_4 and 2 mM KH_2PO_4, pH 7.4), 10 μL of RBB-labeled PG and 4 μM lysozyme (hen egg white, Sigma) or His_6-RlpA (as indicated). Reactions were incubated for 18 hours at 30° or 37°C, then stopped by centrifugation at 18,000 × g for 10 minutes. (We did not boil reaction mixtures because we found that caused a little bit of dye-release and thus interfered with measuring low activities.) The supernatants were removed and their absorbance was measured at 595 nm using a Beckman Coulter DU60 Spectrophotometer. To test whether limited digestion with an amidase potentiated subsequent digestion by His_6-RlpA, we first subjected dye-labeled sacculi from wild-type *E. coli* to a limited digestion with His_6-AmiD. Reaction mixtures (1 mL) contained PBS buffer, 300 μL of RBB-PG, and 1 μM His_6-AmiD. Digestion was allowed to proceed for 18 hours at 37°C, and then terminated by heating to 95°C for 10 min. Sacculi were recovered by centrifugation and washed repeatedly with water until the supernatants were colorless (~4 washes). His_6-AmiD-treated RBB-PG was then suspended in 300 μL water, and used in assays as described above. As controls, sacculi were digested overnight with 1 μM His_6-RlpA or protein was omitted.

Muropeptide analysis of PG hydrolase reactions

Sacculi were incubated with wild type or mutant His_6-RlpA protein (4 μM) for 2 hours at 37°C in PBS. Reactions were terminated by heating to 95°C for 5 minutes. Reaction mixtures were centrifuged at 18,000 × g for 15 minutes and the supernatant was separated from the pellet. The PG in both fractions was then prepared for high-performance liquid chromatography (HPLC) as described (Popham *et al.*, 1996a). Purified muropeptides were identified by amino acid/amino sugar analyses and mass spectrometry as previously described (Popham *et al.*, 1996b).

Western blotting

Western blotting was performed as previously described (Arends *et al.*, 2010). Briefly, cells from 1 mL of culture grown to an OD_{600} ~0.5 were centrifuged, resuspended in 200 μL of Laemmli sample buffer containing 5% β-mercaptoethanol and boiled for 10 minutes. 10 μL aliquots were subjected to a SDS-PAGE (10% polyacrylamide). Proteins were transferred onto nitrocellulose membranes and detected using standard methods. Rabbit anti-RFP serum (a gift from L. Shapiro) was used at a 1:10,000 dilution. The secondary antibody (used at a 1:8,000 dilution) was horseradish peroxidase-conjugated goat anti-rabbit antibody (Thermo Scientific) and detection was with SuperSignal West Pico Chemiluminescent Substrate (Thermo Scientific). Blots were visualized using a Fujifilm LAS-1000 imager.

Supplementary Material

Refer to Web version on PubMed Central for supplementary material.

Acknowledgments

This paper is dedicated to the memory of Sydney Kustu. We thank Tim Yahr and Mark Urbanowski for access to the PA14 Tn library and help with *P. aeruginosa* genetics, Lucy Shapiro for anti-mCherry serum, Rich Helm in the Virginia Tech Mass Spectrometry Incubator for help in interpreting fragmentation patterns, Jianqiang Shao of The

University of Iowa Central Microscopy Core Facility for help with FLIP and scanning electron microscopy, Lokesh Gakhar of The University of Iowa Protein Crystallography Facility for help with molecular modeling, Andy Thunnissen for information on EmtA/MltE, and Tom Bernhardt for pET28a-AmiD. We are grateful to past and present members of the Weiss lab (N. Handler, T. Duncan, M. Morabe, and E. Ransom) for technical assistance and discussions. M. Morabe was a participant in the summer program “REU in Microbiology at The University of Iowa” supported by NSF DBI 7290775. Research reported in this publication was supported by the National Institute of Allergy and Infectious Disease of the National Institutes of Health under award number R21AI088298 to D.L.P. and GM083975 to D.S.W. The content is solely the responsibility of the authors and does not necessarily represent the official views of the National Institutes of Health.

References

Abanes-De Mello A, Sun YL, Aung S, Pogliano K. A cytoskeleton-like role for the bacterial cell wall during engulfment of the *Bacillus subtilis* forespore. Genes Dev. 2002; 16:3253–3264. [PubMed: 12502745]

Arends SJ, Williams K, Scott RJ, Rolong S, Popham DL, Weiss DS. Discovery and characterization of three new *Escherichia coli* septal ring proteins that contain a SPOR domain: DamX, DedD, and RlpA. J Bacteriol. 2010; 192:242–255. [PubMed: 19880599]

Artola-Recolons C, Carrasco-Lopez C, Llarrull LI, Kumarasiri M, Lastochkin E, Martinez de Ilarduya I, Meindl K, Uson I, Mobashery S, Hermoso JA. High-resolution crystal structure of MltE, an outer membrane-anchored endolytic peptidoglycan lytic transglycosylase from *Escherichia coli*. Biochemistry. 2011; 50:2384–2386. [PubMed: 21341761]

Banzhaf M, van den Berg van Saparoea B, Terrak M, Fraipont C, Egan A, Philippe J, Zapun A, Breukink E, Nguyen-Disteche M, den Blaauwen T, Vollmer W. Cooperativity of peptidoglycan synthases active in bacterial cell elongation. Mol Microbiol. 2012; 85:179–194. [PubMed: 22606933]

Bernhardt TG, de Boer PA. The *Escherichia coli* amidase AmiC is a periplasmic septal ring component exported via the twin-arginine transport pathway. Mol Microbiol. 2003; 48:1171–1182. [PubMed: 12787347]

Blackburn NT, Clarke AJ. Characterization of soluble and membrane-bound family 3 lytic transglycosylases from *Pseudomonas aeruginosa*. Biochemistry. 2002; 41:1001–1013. [PubMed: 11790124]

Castillo RM, Mizuguchi K, Dhanaraj V, Albert A, Blundell TL, Murzin AG. A six-stranded double-psi beta barrel is shared by several protein superfamilies. Structure. 1999; 7:227–236. [PubMed: 10368289]

Cavallari JF, Lamers RP, Scheurwater EM, Matos AL, Burrows LL. Changes to its peptidoglycan-remodeling enzyme repertoire modulate beta-lactam resistance in *Pseudomonas aeruginosa*. Antimicrob Agents Chemother. 2013; 57:3078–3084. [PubMed: 23612194]

Chaput C, Labigne A, Boneca IG. Characterization of *Helicobacter pylori* lytic transglycosylases Slt and MltD. J Bacteriol. 2007; 189:422–429. [PubMed: 17085576]

Chastanet A, Losick R. Engulfment during sporulation in *Bacillus subtilis* is governed by a multi-protein complex containing tandemly acting autolysins. Mol Microbiol. 2007; 64:139–152. [PubMed: 17376078]

Cloud KA, Dillard JP. Mutation of a single lytic transglycosylase causes aberrant septation and inhibits cell separation of *Neisseria gonorrhoeae*. J Bacteriol. 2004; 186:7811–7814. [PubMed: 15516597]

Davies DG, Parsek MR, Pearson JP, Iglewski BH, Costerton JW, Greenberg EP. The involvement of cell-to-cell signals in the development of a bacterial biofilm. Science. 1998; 280:295–298. [PubMed: 9535661]

Dörr T, Cava F, Lam H, Davis BM, Waldor MK. Substrate specificity of an elongation-specific peptidoglycan endopeptidase and its implications for cell wall architecture and growth of *Vibrio cholerae*. Mol Microbiol. 2013; 89:949–962. [PubMed: 23834664]

Fibriansah G, Gliubich FI, Thunnissen AM. On the mechanism of peptidoglycan binding and cleavage by the endo-specific lytic transglycosylase MltE from *Escherichia coli*. Biochemistry. 2012; 51:9164–9177. [PubMed: 23075328]

Gan L, Chen S, Jensen GJ. Molecular organization of Gram-negative peptidoglycan. Proc Natl Acad Sci USA. 2008; 105:18953–18957. [PubMed: 19033194]

Gerding MA, Liu B, Bendezu FO, Hale CA, Bernhardt TG, de Boer PA. Self-enhanced accumulation of FtsN at Division Sites and Roles for Other Proteins with a SPOR domain (DamX, DedD, and RlpA) in *Escherichia coli* cell constriction. J Bacteriol. 2009; 191:7383–7401. [PubMed: 19684127]

Gilmore ME, Bandyopadhyay D, Dean AM, Linnstaedt SD, Popham DL. Production of muramic delta-lactam in *Bacillus subtilis* spore peptidoglycan. J Bacteriol. 2004; 186:80–89. [PubMed: 14679227]

Gode-Potratz CJ, Kustusch RJ, Breheny PJ, Weiss DS, McCarter LL. Surface sensing in *Vibrio parahaemolyticus* triggers a programme of gene expression that promotes colonization and virulence. Mol Microbiol. 2011; 79:240–263. [PubMed: 21166906]

Gutierrez J, Smith R, Pogliano K. SpoIID-mediated peptidoglycan degradation is required throughout engulfment during *Bacillus subtilis* sporulation. J Bacteriol. 2010; 192:3174–3186. [PubMed: 20382772]

Hashimoto M, Ooiwa S, Sekiguchi J. Synthetic lethality of the *lytE cwlO* genotype in *Bacillus subtilis* is caused by lack of D,L-endopeptidase activity at the lateral cell wall. J Bacteriol. 2012; 194:796–803. [PubMed: 22139507]

Heidrich C, Templin MF, Ursinus A, Merdanovic M, Berger J, Schwarz H, de Pedro MA, Höltje JV. Involvement of N-acetylmuramyl-l-alanine amidases in cell separation and antibiotic-induced autolysis of *Escherichia coli*. Mol Microbiol. 2001; 41:167–178. [PubMed: 11454209]

Heidrich C, Ursinus A, Berger J, Schwarz H, Höltje JV. Effects of multiple deletions of murein hydrolases on viability, septum cleavage, and sensitivity to large toxic molecules in *Escherichia coli*. J Bacteriol. 2002; 184:6093–6099. [PubMed: 12399477]

Höltje JV, Mirelman D, Sharon N, Schwarz U. Novel type of murein transglycosylase in *Escherichia coli*. J Bacteriol. 1975; 124:1067–1076. [PubMed: 357]

Hsiao CH, Ueno N, Shao JQ, Schroeder KR, Moore KC, Donelson JE, Wilson ME. The effects of macrophage source on the mechanism of phagocytosis and intracellular survival of *Leishmania*. Microbes Infect. 2011; 13:1033–1044. [PubMed: 21723411]

Jacobs MA, Alwood A, Thaipisuttikul I, Spencer D, Haugen E, Ernst S, Will O, Kaul R, Raymond C, Levy R, Chun-Rong L, Guenthner D, Bovee D, Olson MV, Manoil C. Comprehensive transposon mutant library of *Pseudomonas aeruginosa*. Proc Natl Acad Sci USA. 2003; 100:14339–14344. [PubMed: 14617778]

Kelley LA, Sternberg MJ. Protein structure prediction on the Web: a case study using the Phyre server. Nat Protoc. 2009; 4:363–371. [PubMed: 19247286]

Kerff F, Amoroso A, Herman R, Sauvage E, Petrella S, Filee P, Charlier P, Joris B, Tabuchi A, Nikolaidis N, Cosgrove DJ. Crystal structure and activity of *Bacillus subtilis* YoaJ (EXLX1), a bacterial expansin that promotes root colonization. Proc Natl Acad Sci USA. 2008; 105:16876–16881. [PubMed: 18971341]

Kraft AR, Templin MF, Höltje JV. Membrane-bound lytic endotransglycosylase in *Escherichia coli*. J Bacteriol. 1998; 180:3441–3447. [PubMed: 9642199]

Kwok S, Chang SY, Sninsky JJ, Wang A. A guide to the design and use of mismatched and degenerate primers. PCR Methods Appl. 1994; 3:S39–47. [PubMed: 8173508]

Lee M, Hesek D, Llarrull LI, Lastochkin E, Pi H, Boggess B, Mobashery S. Reactions of all *Escherichia coli* lytic transglycosylases with bacterial cell wall. J Am Chem Soc. 2013; 135:3311–3314. [PubMed: 23421439]

Legaree BA, Clarke AJ. Interaction of penicillin-binding protein 2 with soluble lytic transglycosylase B1 in *Pseudomonas aeruginosa*. J Bacteriol. 2008; 190:6922–6926. [PubMed: 18708507]

Liberati NT, Urbach JM, Miyata S, Lee DG, Drenkard E, Wu G, Villanueva J, Wei T, Ausubel FM. An ordered, nonredundant library of *Pseudomonas aeruginosa* strain PA14 transposon insertion mutants. Proc Natl Acad Sci USA. 2006; 103:2833–2838. [PubMed: 16477005]

Matsuzawa H, Asoh S, Kunai K, Muraiso K, Takasuga A, Ohta T. Nucleotide sequence of the rodA gene, responsible for the rod shape of *Escherichia coli: rodA* and the *pbpA* gene, encoding penicillin-binding protein 2, constitute the *rodA* operon. J Bacteriol. 1989; 171:558–560. [PubMed: 2644207]

Mercer KL, Weiss DS. The *Escherichia coli* cell division protein FtsW is required to recruit its cognate transpeptidase, FtsI (PBP3), to the division site. J Bacteriol. 2002; 184:904–912. [PubMed: 11807049]

Mishima M, Shida T, Yabuki K, Kato K, Sekiguchi J, Kojima C. Solution structure of the peptidoglycan binding domain of *Bacillus subtilis* cell wall lytic enzyme CwlC: characterization of the sporulation-related repeats by NMR. Biochemistry. 2005; 44:10153–10163. [PubMed: 16042392]

Mohammadi T, van Dam V, Sijbrandi R, Vernet T, Zapun A, Bouhss A, Diepeveen-de Bruin M, Nguyen-Distèche M, de Kruijff B, Breukink E. Identification of FtsW as a transporter of lipid-linked cell wall precursors across the membrane. EMBO J. 2011; 30:1425–1432. [PubMed: 21386816]

Möll A, Thanbichler M. FtsN-like proteins are conserved components of the cell division machinery in proteobacteria. Mol Microbiol. 2009; 72:1037–1053. [PubMed: 19400794]

Monteiro C, Fang X, Ahmad I, Gomelsky M, Romling U. Regulation of biofilm components in *Salmonella enterica* serovar Typhimurium by lytic transglycosylases involved in cell wall turnover. J Bacteriol. 2011; 193:6443–6451. [PubMed: 21965572]

Morlot C, Uehara T, Marquis KA, Bernhardt TG, Rudner DZ. A highly coordinated cell wall degradation machine governs spore morphogenesis in *Bacillus subtilis*. Genes Dev. 2010; 24:411–422. [PubMed: 20159959]

Moynie L, Schnell R, McMahon SA, Sandalova T, Boulkerou WA, Schmidberger JW, Alphey M, Cukier C, Duthie F, Kopec J, Liu H, Jacewicz A, Hunter WN, Naismith JH, Schneider G. The AEROPATH project targeting *Pseudomonas aeruginosa*: crystallographic studies for assessment of potential targets in early-stage drug discovery. Acta Crystallogr Sect F Struct Biol Cryst Commun. 2013; 69:25–34.

Newman JR, Fuqua C. Broad-host-range expression vectors that carry the L-arabinose-inducible *Escherichia coli araBAD* promoter and the *araC* regulator. Gene. 1999; 227:197–203. [PubMed: 10023058]

Nikolaidis I, Izore T, Job V, Thielens N, Breukink E, Dessen A. Calcium-dependent complex formation between PBP2 and lytic transglycosylase SltB1 of *Pseudomonas aeruginosa*. Microb Drug Resist. 2012; 18:298–305. [PubMed: 22432706]

Peters NT, Dinh T, Bernhardt TG. A fail-safe mechanism in the septal ring assembly pathway generated by the sequential recruitment of cell separation amidases and their activators. J Bacteriol. 2011; 193:4973–4983. [PubMed: 21764913]

Pogliano K, Harry E, Losick R. Visualization of the subcellular location of sporulation proteins in *Bacillus subtilis* using immunofluorescence microscopy. Mol Microbiol. 1995; 18:459–470. [PubMed: 8748030]

Popham DL, Helin J, Costello CE, Setlow P. Analysis of the peptidoglycan structure of *Bacillus subtilis* endospores. J Bacteriol. 1996a; 178:6451–6458. [PubMed: 8932300]

Popham DL, Helin J, Costello CE, Setlow P. Muramic lactam in peptidoglycan of *Bacillus subtilis* spores is required for spore outgrowth but not for spore dehydration or heat resistance. Proc Natl Acad Sci USA. 1996b; 93:15405–15410. [PubMed: 8986824]

Potluri LP, de Pedro MA, Young KD. *Escherichia coli* low-molecular-weight penicillin-binding proteins help orient septal FtsZ, and their absence leads to asymmetric cell division and branching. Mol Microbiol. 2012; 84:203–224. [PubMed: 22390731]

Powell AJ, Liu ZJ, Nicholas RA, Davies C. Crystal structures of the lytic transglycosylase MltA from *N.gonorrhoeae* and *E.coli*: insights into interdomain movements and substrate binding. J Mol Biol. 2006; 359:122–136. [PubMed: 16618494]

Priyadarshini R, de Pedro MA, Young KD. Role of peptidoglycan amidases in the development and morphology of the division septum in *Escherichia coli*. J Bacteriol. 2007; 189:5334–5347. [PubMed: 17483214]

Punta M, Coggill PC, Eberhardt RY, Mistry J, Tate J, Boursnell C, Pang N, Forslund K, Ceric G, Clements J, Heger A, Holm L, Sonnhammer EL, Eddy SR, Bateman A, Finn RD. The Pfam protein families database. Nucleic Acids Res. 2012; 40:D290–301. [PubMed: 22127870]

Rietsch A, Vallet-Gely I, Dove SL, Mekalanos JJ. ExsE, a secreted regulator of type III secretion genes in *Pseudomonas aeruginosa*. Proc Natl Acad Sci USA. 2005; 102:8006–8011. [PubMed: 15911752]

Romeis T, Vollmer W, Höltje JV. Characterization of three different lytic transglycosylases in *Escherichia coli*. FEMS Microbiol Lett. 1993; 111:141–146. [PubMed: 8405923]

Sampedro J, Cosgrove DJ. The expansin superfamily. Genome Biol. 2005; 6:242. [PubMed: 16356276]

Scheurwater E, Reid CW, Clarke AJ. Lytic transglycosylases: bacterial space-making autolysins. Int J Biochem Cell Biol. 2008; 40:586–591. [PubMed: 17468031]

Scheurwater EM, Pfeffer JM, Clarke AJ. Production and purification of the bacterial autolysin *N*-acetylmuramoyl-l-alanine amidase B from *Pseudomonas aeruginosa*. Protein Expr Purif. 2007; 56:128–137. [PubMed: 17723308]

Schweizer HP. Allelic exchange in *Pseudomonas aeruginosa* using novel ColE1-type vectors and a family of cassettes containing a portable oriT and the counter-selectable *Bacillus subtilis* sacB marker. Mol Microbiol. 1992; 6:1195–1204. [PubMed: 1588818]

Sievers F, Wilm A, Dineen D, Gibson TJ, Karplus K, Li W, Lopez R, McWilliam H, Remmert M, Soding J, Thompson JD, Higgins DG. Fast, scalable generation of high-quality protein multiple sequence alignments using Clustal Omega. Mol Syst Biol. 2011; 7:539. [PubMed: 21988835]

Singh SK, SaiSree L, Amrutha RN, Reddy M. Three redundant murein endopeptidases catalyse an essential cleavage step in peptidoglycan synthesis of *Escherichia coli* K12. Mol Microbiol. 2012; 86:1036–1051. [PubMed: 23062283]

Tarry M, Arends SJ, Roversi P, Piette E, Sargent F, Berks BC, Weiss DS, Lea SM. The *Escherichia coli* cell division protein and model Tat substrate SufI (FtsP) localizes to the septal ring and has a multicopper oxidase-like structure. J Mol Biol. 2009; 386:504–519. [PubMed: 19135451]

Turner RD, Hurd AF, Cadby A, Hobbs JK, Foster SJ. Cell wall elongation mode in Gram-negative bacteria is determined by peptidoglycan architecture. Nat Commun. 2013; 4:1496. [PubMed: 23422664]

Uehara T, Bernhardt TG. More than just lysins: peptidoglycan hydrolases tailor the cell wall. Curr Opin Microbiol. 2011; 14:698–703. [PubMed: 22055466]

Uehara T, Park JT. An anhydro-*N*-acetylmuramyl-l-alanine amidase with broad specificity tethered to the outer membrane of *Escherichia coli*. J Bacteriol. 2007; 189:5634–5641. [PubMed: 17526703]

Uehara T, Parzych KR, Dinh T, Bernhardt TG. Daughter cell separation is controlled by cytokinetic ring-activated cell wall hydrolysis. EMBO J. 2010; 29:1412–1422. [PubMed: 20300061]

Ursinus A, Höltje JV. Purification and properties of a membrane-bound lytic transglycosylase from *Escherichia coli*. J Bacteriol. 1994; 176:338–343. [PubMed: 8288527]

Ursinus A, van den Ent F, Brechtel S, de Pedro M, Höltje JV, Löwe J, Vollmer W. Murein (peptidoglycan) binding property of the essential cell division protein FtsN from *Escherichia coli*. J Bacteriol. 2004; 186:6728–6737. [PubMed: 15466024]

van Heijenoort J. Peptidoglycan hydrolases of *Escherichia coli*. Microbiol Mol Biol Rev. 2011; 75:636–663. [PubMed: 22126997]

van Straaten KE, Barends TR, Dijkstra BW, Thunnissen AM. Structure of *Escherichia coli* Lytic transglycosylase MltA with bound chitohexaose: implications for peptidoglycan binding and cleavage. J Biol Chem. 2007; 282:21197–21205. [PubMed: 17502382]

van Straaten KE, Dijkstra BW, Vollmer W, Thunnissen AM. Crystal structure of MltA from *Escherichia coli* reveals a unique lytic transglycosylase fold. J Mol Biol. 2005; 352:1068–1080. [PubMed: 16139297]

Vollmer W, Blanot D, de Pedro MA. Peptidoglycan structure and architecture. FEMS Microbiol Rev. 2008a; 32:149–167. [PubMed: 18194336]

Vollmer W, Höltje JV. The architecture of the murein (peptidoglycan) in gram-negative bacteria: vertical scaffold or horizontal layer(s)? J Bacteriol. 2004; 186:5978–5987. [PubMed: 15342566]

Vollmer W, Joris B, Charlier P, Foster S. Bacterial peptidoglycan (murein) hydrolases. FEMS Microbiol Rev. 2008b; 32:259–286. [PubMed: 18266855]

Warth AD, Strominger JL. Structure of the peptidoglycan of bacterial spores: occurrence of the lactam of muramic acid. Proc Natl Acad Sci USA. 1969; 64:528–535. [PubMed: 4982357]

Winsor GL, Lam DK, Fleming L, Lo R, Whiteside MD, Yu NY, Hancock RE, Brinkman FS. *Pseudomonas* Genome Database: improved comparative analysis and population genomics capability for *Pseudomonas* genomes. Nucleic Acids Res. 2011; 39:D596–600. [PubMed: 20929876]

Yang DC, Peters NT, Parzych KR, Uehara T, Markovski M, Bernhardt TG. An ATP-binding cassette transporter-like complex governs cell-wall hydrolysis at the bacterial cytokinetic ring. Proc Natl Acad Sci USA. 2011; 108:E1052–1060. [PubMed: 22006326]

Yang DC, Tan K, Joachimiak A, Bernhardt TG. A conformational switch controls cell wall-remodelling enzymes required for bacterial cell division. Mol Microbiol. 2012; 85:768–781. [PubMed: 22715947]

Zhou R, Chen S, Recsei P. A dye release assay for determination of lysostaphin activity. Anal Biochem. 1988; 171:141–144. [PubMed: 3407910]

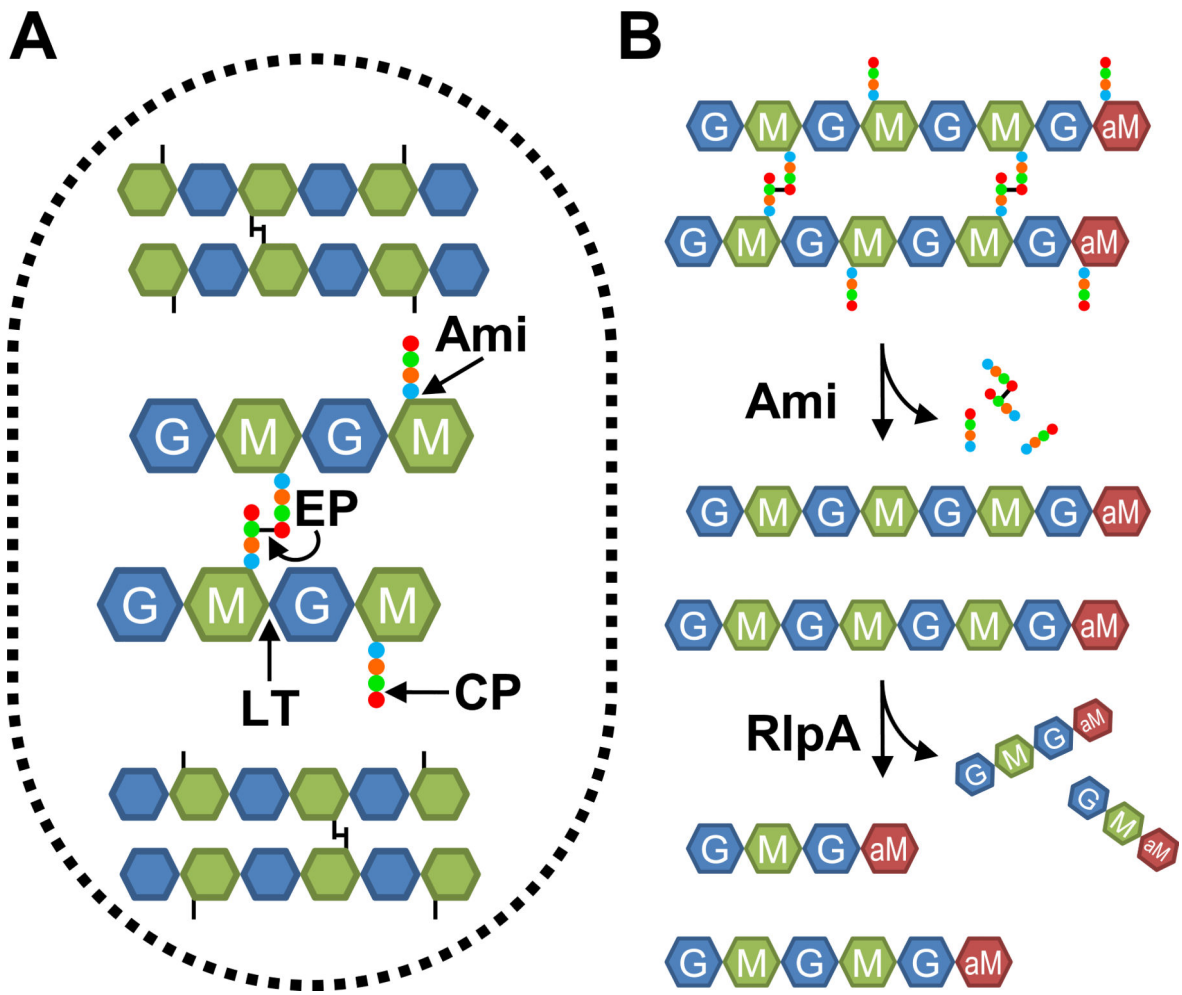

Figure 1.

(A) Cartoon of the PG sacculus. Glycan strands run roughly perpendicular to the long axis of the cell and are composed of a β-1,4-linked NAG (G) and NAM (M). Short peptides (circles) are attached to the NAM residues and cross-link the glycan strands. Lytic transglycosylases (LT) cleave the β-1,4 glucosidic bonds. Amidases (Ami) remove the stem peptides from the NAM residues. Endopeptidases (EP) cleave the peptide cross-links. Carboxypeptidases (CP) remove terminal amino acids from the stem peptides. (B) Model for sequential degradation of PG by amidases and RlpA. First, amidases remove stem peptides from glycan strands. Then RlpA cleaves the glycan strands, releasing mainly tetra- and hexasaccharides with a 1,6-anhydroNAM end (aM).

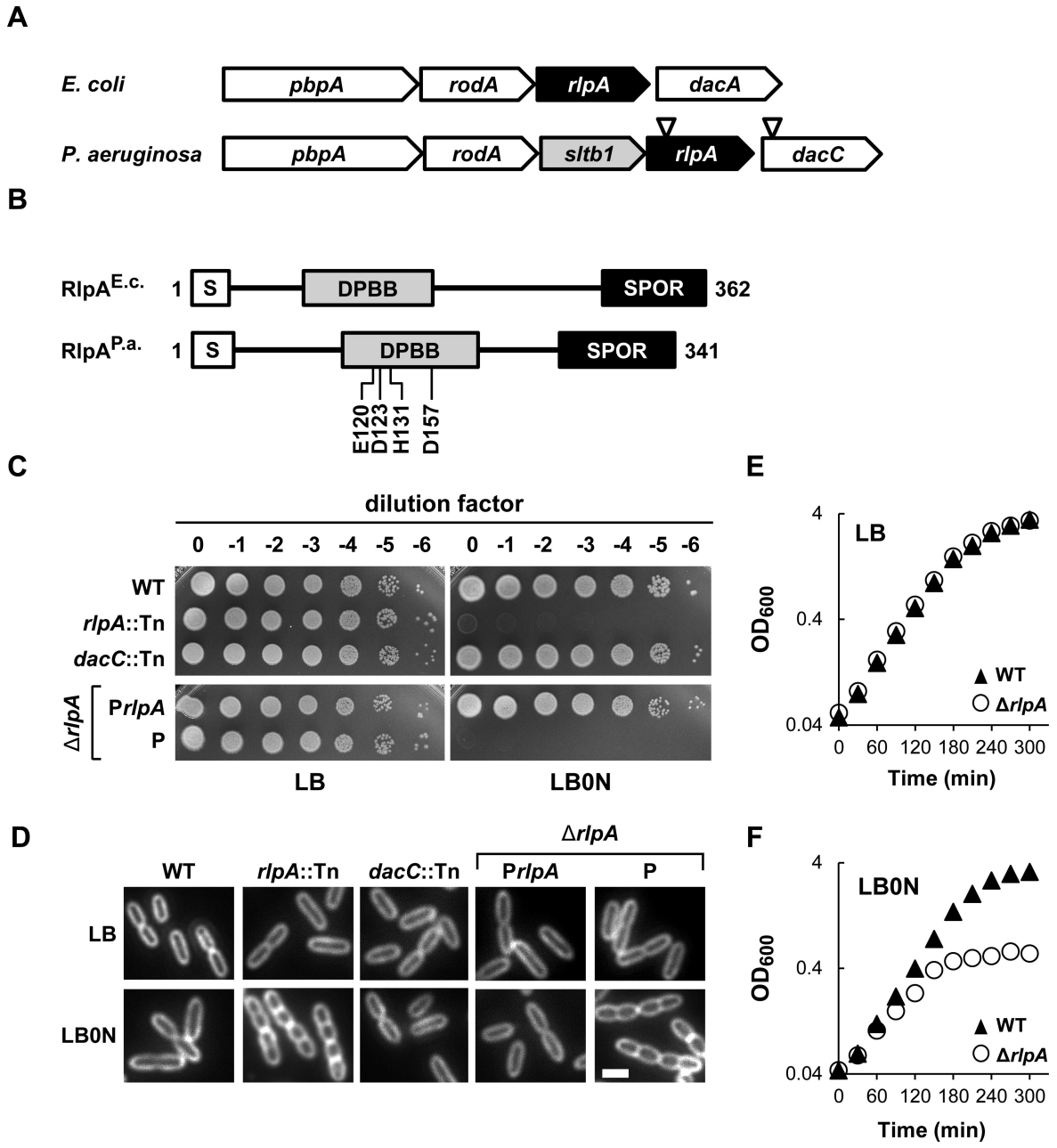

Figure 2. Growth and chaining of an *rlpA* mutant

(A) *rlpA* loci from *E. coli* K-12 and *P. aeruginosa* UCBPP-PA14. Inverted triangles depict relative positions of the MAR2xT7 transposon in *rlpA* and *dacC*. PBPA is a transpeptidase needed for cross-linking PG, especially during elongation. RodA is considered to be a flippase that transports lipid-linked disaccharide-pentapeptide precursors to the periplasm for PG synthesis during elongation. DacA is a PG carboxypeptidase. SltB1 is a soluble lytic transglycosylase found in the periplasm. DacC is a PG carboxypeptidase more closely related to DacC of *E. coli* than to DacA of *E. coli*. (B) Schematic diagram of the domain architecture of RlpA. S, type II signal sequence. DPBB, RlpA-like double psi beta barrel domain. SPOR, SPOR domain. DPBB domain residues targeted for mutagenesis are shown

below the *P. aeruginosa* protein. (C) Plating efficiency. Tenfold serial dilutions of cells with the indicated genotypes were spotted onto LB (left) or LB0N (right). Plates were photographed after incubation overnight at 37°C. P refers to the empty vector (pJN105), while P*rlpA* refers to a derivative (pDSW1398) that carries *rlpA*. (D) Division phenotypes. Cells grown at 37°C in LB or LB0N to an OD_{600} ~0.5 were fixed, stained with the membrane dye FM4-64 and photographed under fluorescence. The white bar represents 2 μm. (D) Growth curves for wild type and the Δ*rlpA* mutant grown in LB or LB0N at 37°C. Strains shown are MJ1 (WT), MJ7 (*rlpA*::Tn), MJ18 (*dacC*::Tn), MJ27 (Δ*rlpA*/P*rlpA*), MJ26 (Δ*rlpA*/P) and MJ24 (Δ*rlpA*).

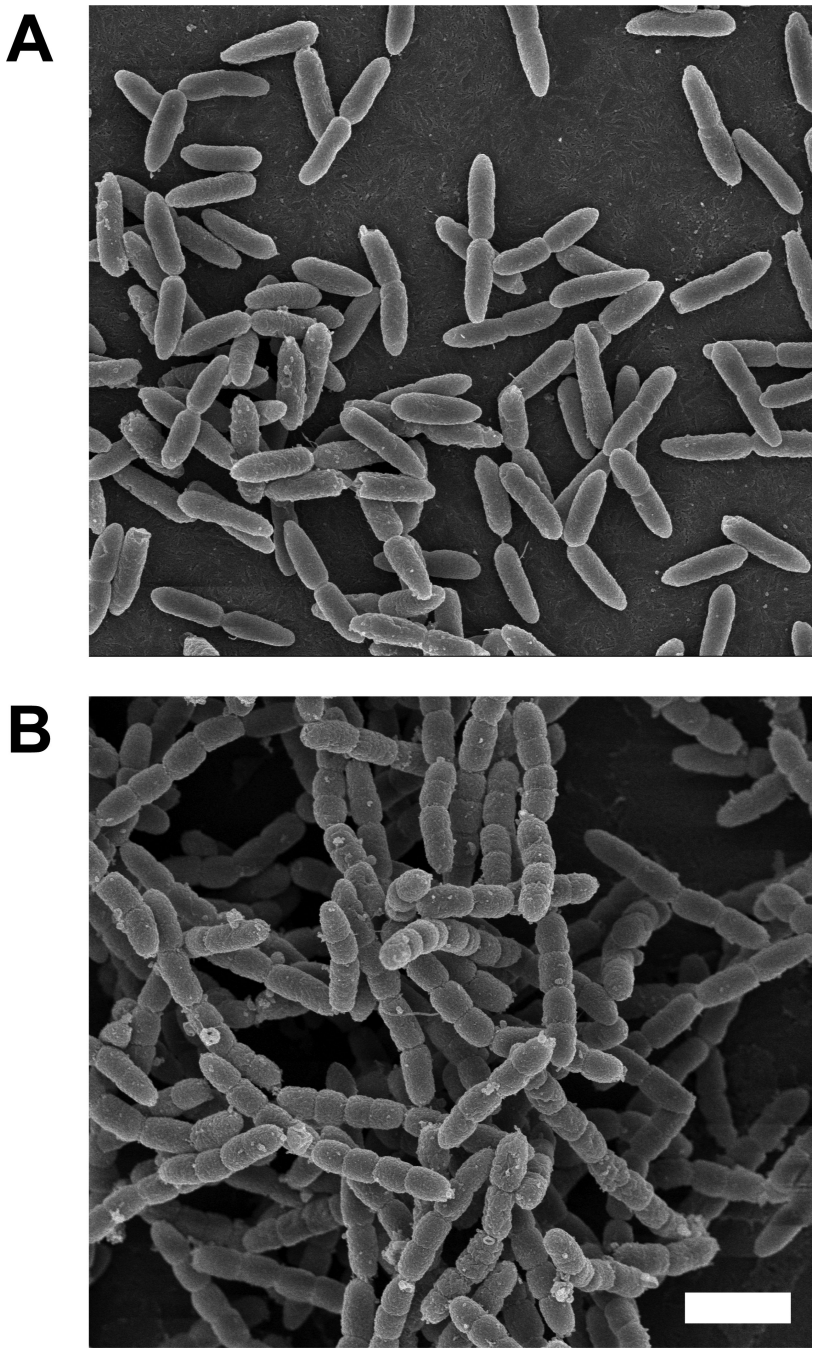

Figure 3. Scanning electron microscopy of a Δ*rlpA* mutant of *P. aeruginosa*

Wild type strain MJ1(A) and Δ*rlpA* strain MJ24 (B) were grown at 37°C in LB0N from an OD_{600} ~0.1 to an OD_{600} ~0.7, then fixed and prepared for SEM. The white bar represents 2 μm.

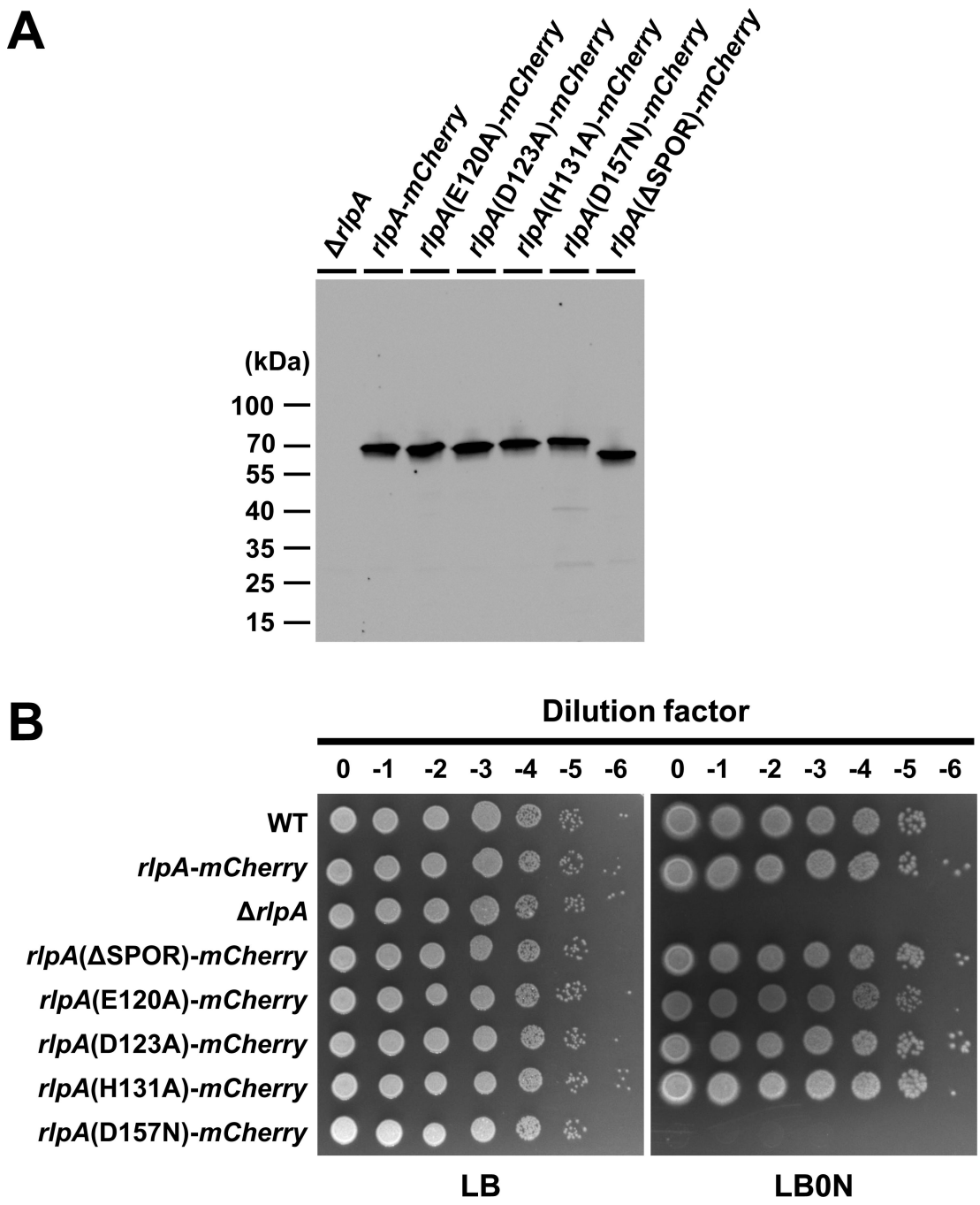

Figure 4. Phenotypes of *rlpA* mutants with a SPOR domain deletion or lesions in the DPBB domain

(A) Western blot with anti-mCherry sera. Size markers are indicated to the left of the blot. The predicted masses are 61 kDa for RlpA-mCherry and 53 kDa for RlpA(ΔSPOR)-mCherry, assuming removal of the signal sequence. (B) Plating efficiency, as in Figure 2. The strains shown are MJ1 (WT), MJ36 (*rlpA-mCherry*), MJ24 (Δ*rlpA*), MJ42 (ΔSPOR), MJ81 (E120A), MJ83 (D123A), MJ85 (H131A) and MJ89 (D157N).

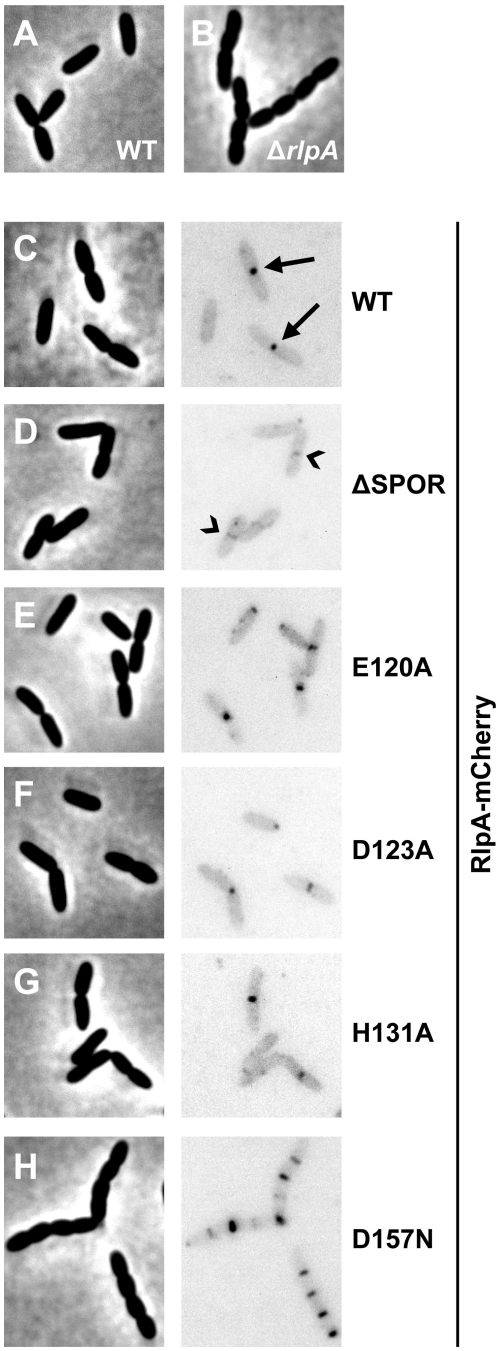

Figure 5. Function and localization of mutant derivatives of RlpA

Strains grown in LB0N at 37°C to an OD_{600} ~0.5 were imaged by phase-contrast (left) and fluorescence (right) microscopy. The fluorescence micrographs were inverted to better visualize localization of mCherry fusion proteins. Arrows in (C) point to septal localization of RlpA-mCherry. Chevrons in (D) point to sites with faint septal localization of RlpA(ΔSPOR)-mCherry. The strains shown are listed in the legend to Figure 4.

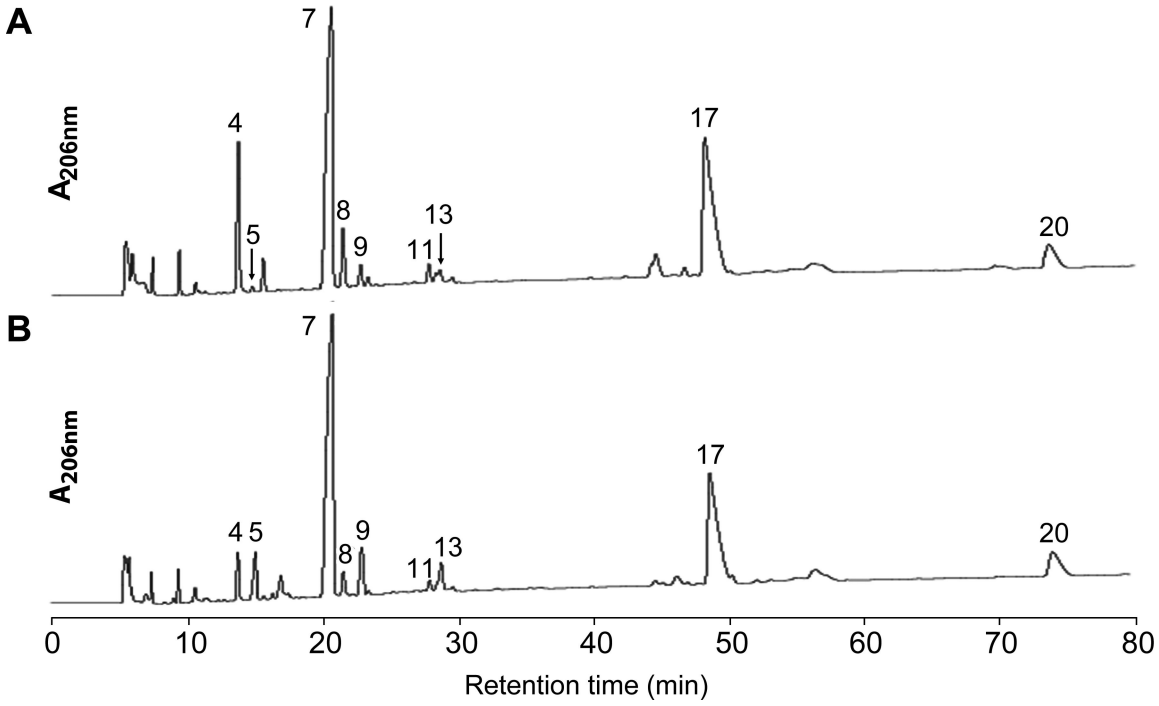

Figure 6. Δ*rlpA* has PG alterations as compared to wild type

HPLC elution profiles of muropeptides from WT (A) and Δ*rlpA* (B). PG sacculi were isolated from strains MJ1 (WT) and MJ24 (Δ*rlpA*) that had been grown to an OD_{600} ~0.5 in LB0N. Sacculi were digested with mutanolysin and the resulting muropeptides were reduced with borohydride prior to loading onto an RP-HPLC column. Muropeptide peaks are numbered and were identified by amino acid and amino sugar analysis (Table S2) and tandem mass spectrometry (Table S3). Arrows in (A) point to small peaks that are difficult to see.

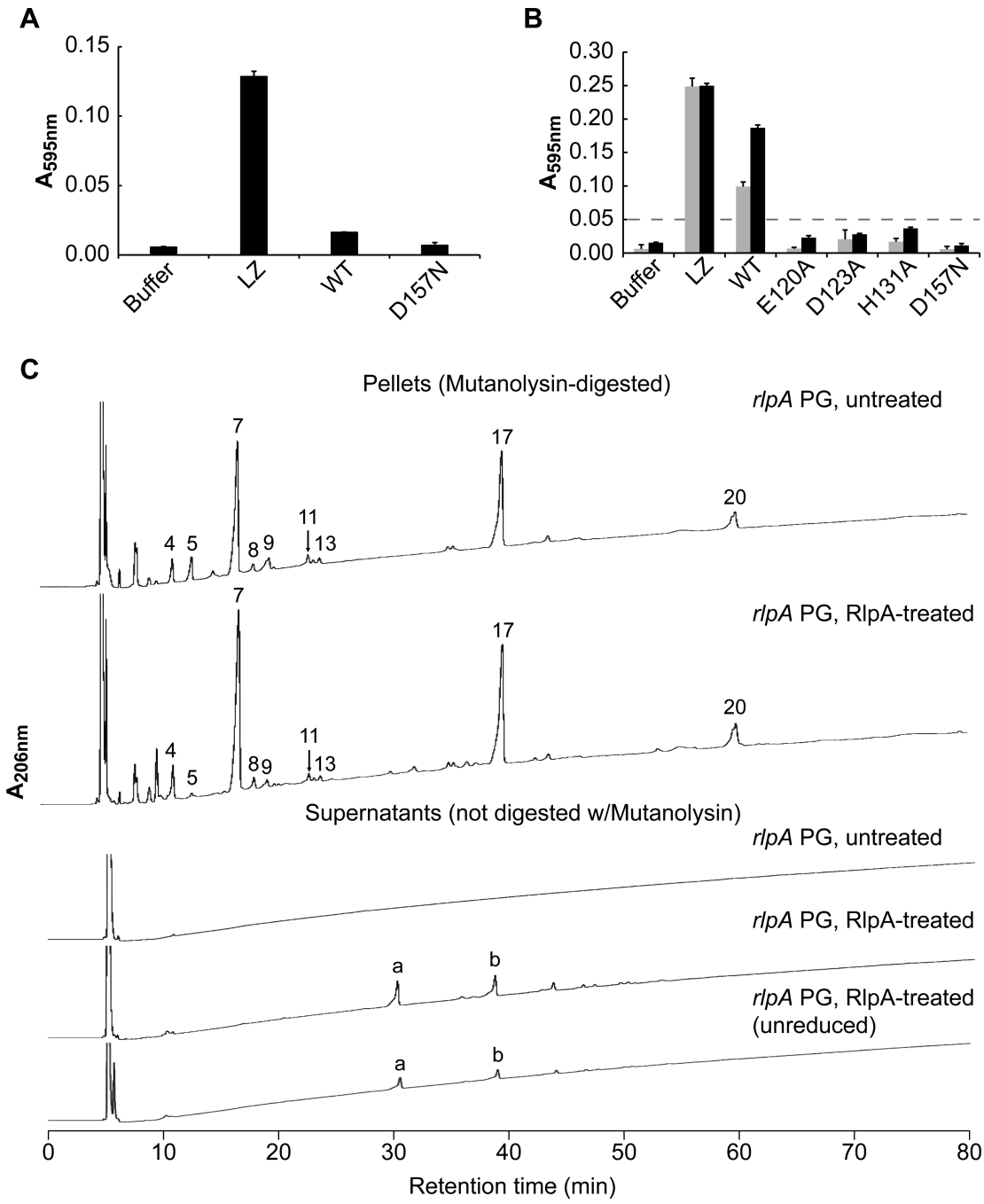

Figure 7. RlpA is a lytic transglycosylase that cleaves naked glycan strands

(A) Purified His_6-RlpA does not solubilize dye-labeled PG sacculi from WT cells. Reaction mixtures contained 4 μM protein and were incubated 18 hours at 37°C. Lysozyme (LZ) served as a positive control. WT = His_6-RlpA. D157N = His_6-RlpA with a D157N amino acid substitution. Data shown are mean and standard deviation of a representative experiment done in triplicate. All experiments were done on at least 3 occasions using independent preparations of dye-labeled PG, but because of the different extents of dye-labeling, the data were not pooled. (B) Purified His_6-RlpA solubilizes dye-labeled PG

sacculi from a Δ*rlpA* mutant. Reaction conditions as above except that incubation was at 30°C for 2 hours (grey bars) or 18 hours (black bars). E120A, D123A, H131A and D157N are amino acid substitutions in RlpA. The dashed line at 0.05 AU is provided to facilitate comparison of the mutant proteins. (C) Identification of small PG fragments released by His_6-RlpA. Unlabeled PG sacculi from a Δ*rlpA* mutant were incubated with buffer (untreated) or His_6-RlpA (RlpA-treated). Reaction mixtures were centrifuged to separate residual insoluble PG pellets from soluble PG fragments released into the supernatant. The pellet and supernatant fractions were analyzed by reverse-phase HPLC. Peaks eluting from the HPLC column are numbered as in Figure 6, except for two unique peaks labeled “a” and “b” that were identified by tandem mass spectrometry (Table S4). Unreduced refers to a sample that was not treated with borohydride. All chromatograms are graphed on the same vertical (A_{206} nm) scale.

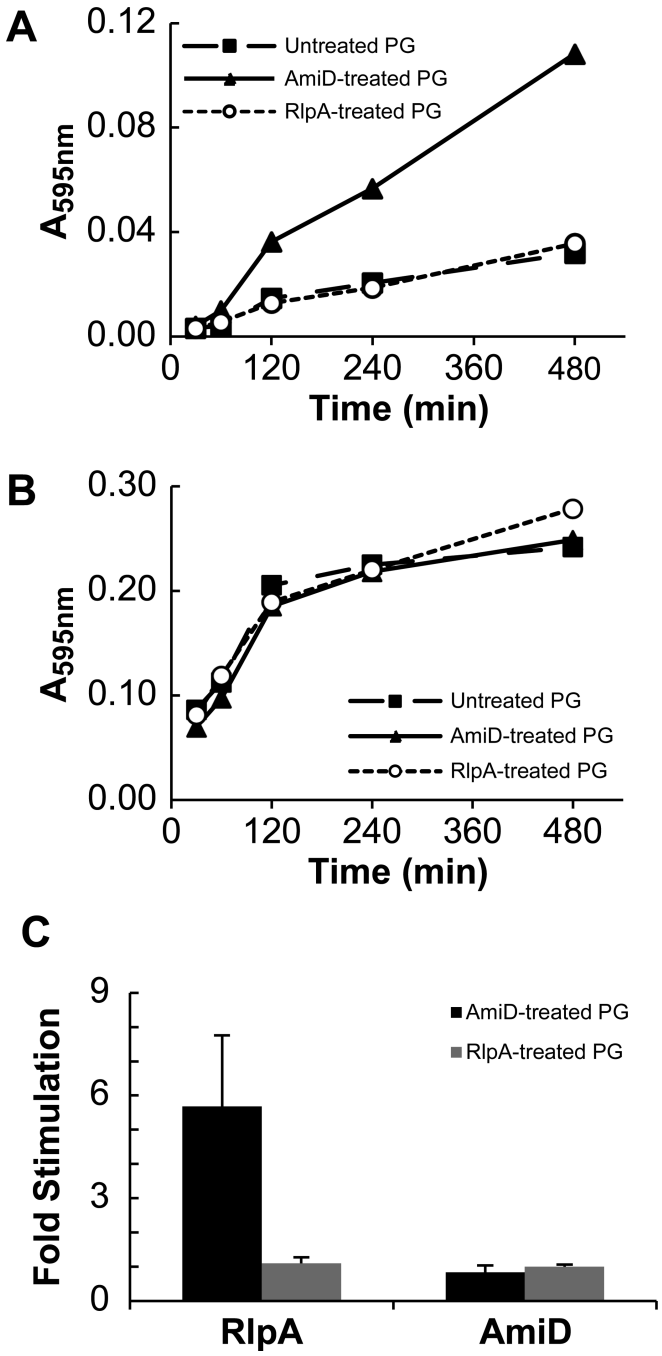

Figure 8. Amidase-treatment of PG renders it susceptible to subsequent cleavage by His_6-RlpA

Dye-labeled sacculi from a wild-type *E. coli* strain were incubated overnight with buffer (as a control; filled squares "untreated"), 1 μM His_6-AmiD (filled triangles) or 1 μM His_6-RlpA (open circles). These substrates were then incubated with 4 μM His_6-RlpA (A) or 4 μM His_6-AmiD (B). A representative experiment is shown with one replicate per time point. (C) Reproducibility of the assay. Dye-release was read after 480 min of incubation as indicated

in (A) and (B). The values shown are the mean and standard deviation of 4 separate experiments done with two preparations of dye-labeled sacculi.

Table 1

Morphological parameters of a mutant lacking *rlpA*

Genotype[a]	NaCl[b]	Avg length μm, (SD)	Avg unit length μm[c]	Avg width μm, (SD)	% Cells with indicated no. of constrictions:			
					0	1	3	>3
WT	+	2.9 (0.7)	2.3	0.9 (0.1)	74	26	0	0
	-	3.1 (0.7)	2.3	0.9 (0.1)	73	27	0	0
Δ *rlpA*	+	3.1 (0.7)	2.4	0.9 (0.1)	75	25	0	0
	-	5.9 (1.9)	1.1	1.1 (0.1)	0	5	66	29

[a] Strains used were MJ1 (WT) and MJ24 *(MpA).* At least 300 cells were evaluated in each case.

[b] Either 1% (+) or 0% (-) NaCl.

[c] The distance between cell poles or constrictions in case of chains of cells.

Table 2

Muropeptide analysis of peptidoglycan from *Pseudomonas aeruginosa* PA14 WT and Δ*rlpA* grown in LB0N

Muropeptide	Structure[b]	Observed *m/z* [M+Na$^+$]	Expected *m/z* [M+Na$^+$]	% of all peaks[c]		% difference
				WT	Δ*rlpA*	
4	DS-Tri	893.5	893.4	8.3 (0.2)	4.4 (1.8)	−47.0
5	TS	999.5	999.3	0.9 (0.6)	2.7 (0.7)	200.0
7	DS-Tetra	964.5	964.4	35.1 (1.2)	39.7 (2.4)	13.1
8	DS-Penta	1021.6	1021.4	3.4 (0.3)	2.0 (0.3)	−41.2
9	HS	1477.7	1478.4	0.9 (0.6)	2.5 (1.2)	177.8
11	DS-Tetra-Tetra	1407.7	1407.6	1.9 (0.6)	1.7 (0.6)	−10.5
13	TS-Tetra	1442.9	1443.4	1.0 (0.2)	1.9 (0.3)	90.0
17	DS-Tetra-DS-Tetra	1888.0	1887.8	27.1 (1.7)	25.1 (2.8)	−7.4
20	DS-Tetra-DS-Tetra anhydro	1868.1	1867.8	4.9 (0.3)	6.4 (0.5)	30.6
Other[a]				16.5	13.6	

[a] "Other" muropeptides includes the summed areas of multiple small peaks that did not show significant variation between the two strains and that were not structurally characterized.

[b] Abbreviations: DS, disaccharide (NAG-NAMol); TS, tetrasaccharide (NAG-NAM-NAG-NAMol); HS, hexasaccharide (NAG-NAM-NAG-NAM-NAG-NAMol). Tri, tripeptide (L-Ala-D-iGlu-m-Dpm); Tetra, tetrapeptide (L-Ala-D-iGlu-m-Dpm-D-Ala); Pent, pentapeptide (L-Ala-D-iGlu-m-Dpm-D-Ala-Gly). Anhydro, 1,6-anhydroNAM. The terminal NAM is in the alcohol form due to borohydride reduction except in the case of anhydro-NAM. [c] Percentages are the mean and standard error of three independent experiments.